BI-TP 96/06
KA-TP-03-96
hep-ph/9602436

How reliably can the Higgs-Boson Mass be predicted from Electroweak Precision Data?[†]

S. Dittmaier, D. Schildknecht

Fakultät für Physik, Universität Bielefeld, D-33615 Bielefeld, Germany

G. Weiglein

Institut für Theoretische Physik, Universität Karlsruhe, D-76128 Karlsruhe, Germany

Revised version
June 1996

Abstract

From the LEP precision data and the measurement of the W-boson mass, upon excluding the observables R_{b}, R_{c} in a combined fit of the top-quark mass, m_{t}, and the Higgs-boson mass, M_{H}, within the Standard Model, we find the weak 1σ bound of $M_{\mathrm{H}} \lesssim 900\,\mathrm{GeV}$. Stronger upper bounds on M_{H}, sometimes presented in the literature, rely heavily on the inclusion of R_{b} in the data sample. Upon including R_{b}, the quality of the fit drastically decreases, and by carefully analyzing the dependence of the fit results on the set of experimental input data we conclude that these stronger bounds are not reliable. Moreover, the stronger bounds on M_{H} are lost if the deviation between theory and experiment in R_{b} is ascribed to contributions of new physics. Replacing $\bar{s}^2_{\mathrm{W}}(\mathrm{LEP})$ by the combined value $\bar{s}^2_{\mathrm{W}}(\mathrm{LEP}+\mathrm{SLD})$ in the data sample leads to a bound of $M_{\mathrm{H}} \lesssim 430\,\mathrm{GeV}$ at the 1σ level. The value of $\bar{s}^2_{\mathrm{W}}(\mathrm{SLD})$ taken alone, however, gives rise to fit results for M_{H} which are in conflict with $M_{\mathrm{H}} \gtrsim 65.2\,\mathrm{GeV}$ from direct searches.

[†]Partially supported by the EC-network contract CHRX-CT94-0579 and the Bundesministerium für Bildung und Forschung, Bonn, Germany.

The discovery [1] of the top quark and the direct determination of its mass of $m_{\rm t}^{\rm exp} = 180 \pm 12\,{\rm GeV}$ open the possibility of improving the constraints on the mass of the Higgs boson, $M_{\rm H}$, from the body of the precision electroweak data at the Z-boson resonance [2, 3] and the experimental value of the W-boson mass, $M_{\rm W}$ [4]. In this note we present our results for $m_{\rm t}$ and $M_{\rm H}$, obtained by performing fits to the precision data and $M_{\rm W}$ within the Standard Model (SM). The dependence of the fits on the experimental data on $R_{\rm b}$, $R_{\rm c}$, and $\bar{s}^2_{\rm W}$ is investigated, and the effects of varying the SM input parameters $\alpha(M_{\rm Z}^2)$ and $\alpha_{\rm s}(M_{\rm Z}^2)$ in the allowed range are discussed. We also examine how the results of these fits are influenced if one allows for non-standard $\rm Z \to b\bar{b}, c\bar{c}$ vertices. Even though several papers on this subject have appeared recently [5, 6, 7], additional investigations combined with comments on the interpretation of the results seem useful.

We start from a global fit to the available electroweak precision data. The large value of $\chi^2_{\rm min}/_{\rm d.o.f.}$, obtained in the fit to be given below, requires a detailed analysis of the impact of different parts of the experimental data. Accordingly, we will subsequently analyze the data in several distinct steps. In a first step we concentrate on the leptonic observables $\Gamma_{\rm l}$ and $\bar{s}^2_{\rm W}({\rm LEP})$, and $M_{\rm W}$ (the set of data to be referred to as "leptonic sector"), and include the total Z-boson width, $\Gamma_{\rm T}$, and the Z-boson width into hadrons, $\Gamma_{\rm h}$, from the set of hadronic observables (referring to this set of data as "all data $\setminus R_{\rm b}, R_{\rm c}$"), thus ignoring in the fits at this stage the partial Z-boson decays $\rm Z \to b\bar{b}, c\bar{c}$. In a second step we include the $\rm Z \to b\bar{b}$ decay mode and determine $m_{\rm t}$ and $M_{\rm H}$ in a fit again. In a third step we finally discuss how the results of the fits change when the decay $\rm Z \to c\bar{c}$ is included, and we also investigate the effect of replacing $\bar{s}^2_{\rm W}({\rm LEP})$ by $\bar{s}^2_{\rm W}({\rm SLD})$ and by the combined value of $\bar{s}^2_{\rm W}({\rm LEP+SLD})$ in the set of data. Within all steps we carry out two alternative fits, a first one in which the Tevatron result of $m_{\rm t}^{\rm exp} = 180 \pm 12$ GeV is included in the fit, and a second one in which $m_{\rm t}$ is treated as a free fit parameter. The procedure adopted obviously allows us to identify the dependence of the results for $m_{\rm t}$ and $M_{\rm H}$ on the set of experimental data used in the fits. The various steps are motivated by the discrepancies [2] between SM prediction and experiment observed in the $\rm Z \to b\bar{b}, c\bar{c}$ decays and the difference between the LEP and SLD results for $\bar{s}^2_{\rm W}$. By including/excluding the experimental information on $m_{\rm t}$ we furthermore investigate how strongly the fit results for $m_{\rm t}$ and $M_{\rm H}$ are correlated. In a final step we discuss fits in which non-standard contributions are allowed.

The set of experimental data is listed in Tab. 1. A subset of the data in Tab. 1 is referred to as "input parameters". This is motivated by the high experimental accuracy of some of the quantities (namely G_μ and $M_{\rm Z}$) and by the non-electroweak origin of others ($\alpha(M_{\rm Z}^2), \alpha_{\rm s}(M_{\rm Z}^2)$). The listed "input parameters" represent the commonly used input for theoretical predictions in the on-shell renormalization scheme. The experimental error of G_μ is entirely negligible with respect to the determination of $m_{\rm t}$ and $M_{\rm H}$. This is also true for $M_{\rm Z}$. For completeness, this was explicitly verified by treating $M_{\rm Z}$ as additional fit parameter. If not otherwise indicated, the parameter $\alpha(M_{\rm Z}^2)$ will be treated as fit parameter employing the constraint of Tab. 1. Finally, we note that the value of $\alpha_{\rm s}(M_{\rm Z}^2)$ given in Tab. 1 is the result from the LEP event shape analysis [2]. Due to the fact that this value disagrees with results from different experiments (e.g. deep-inelastic scattering) and lattice calculations, $\alpha_{\rm s}(M_{\rm Z}^2)$ will either be treated as free fit parameter or the influence of varying $\alpha_{\rm s}(M_{\rm Z}^2)$ as input parameter will be studied separately. For the input parameter $m_{\rm b}$, the mass of the b quark, the value of $m_{\rm b}$ from Tab. 1 will be inserted. A detailed

leptonic sector	hadronic sector	
$\Gamma_\mathrm{l} = 83.93 \pm 0.14\,\mathrm{MeV}$	$R = 20.788 \pm 0.032$	$\Gamma_\mathrm{T} = 2496.3 \pm 3.2\,\mathrm{MeV}$
$\bar{s}^2_\mathrm{W}(\mathrm{LEP}) = 0.23186 \pm 0.00034$	$\sigma_\mathrm{h} = 41.488 \pm 0.078$	$\Gamma_\mathrm{h} = 1744.8 \pm 3.0\,\mathrm{MeV}$
$\bar{s}^2_\mathrm{W}(\mathrm{SLD}) = 0.23049 \pm 0.00050$	$R_\mathrm{b} = 0.2219 \pm 0.0017$	$\Gamma_\mathrm{b} = 387.2 \pm 3.0\,\mathrm{MeV}$
$\bar{s}^2_\mathrm{W}(\mathrm{LEP} + \mathrm{SLD}) = 0.23143 \pm 0.00028$	$R_\mathrm{c} = 0.1543 \pm 0.0074$	$\Gamma_\mathrm{c} = 269 \pm 13\,\mathrm{MeV}$
$M_\mathrm{W} = 80.26 \pm 0.16\,\mathrm{GeV}$		

input parameters
$M_\mathrm{Z} = 91.1884 \pm 0.0022\,\mathrm{GeV}$
$G_\mu = 1.16639(2) \cdot 10^{-5}\,\mathrm{GeV}^{-2}$
$\alpha(M_\mathrm{Z}^2)^{-1} = 128.89 \pm 0.09$
$\alpha_\mathrm{s}(M_\mathrm{Z}^2) = 0.123 \pm 0.006$
$m_\mathrm{b} = 4.5\,\mathrm{GeV}$
$m_\mathrm{t} = 180 \pm 12\,\mathrm{GeV}$

correlation matrices

	σ_h	R	Γ_T
σ_h	1.00	0.15	−0.12
R	0.15	1.00	−0.01
Γ_T	−0.12	−0.01	1.00

	R_b	R_c
R_b	1.00	−0.34
R_c	−0.34	1.00

Table 1: The precision data used in the fits, consisting of the LEP data [2], the SLD value [3] for $\bar{s}^2_\mathrm{W}$, and the world average [4] for M_W. The partial widths Γ_l, Γ_h, Γ_b, and Γ_c are obtained from the observables $R = \Gamma_\mathrm{h}/\Gamma_\mathrm{l}$, $\sigma_\mathrm{h} = (12\pi\Gamma_\mathrm{l}\Gamma_\mathrm{h})/(M_\mathrm{Z}^2\Gamma_\mathrm{T}^2)$, $R_\mathrm{b} = \Gamma_\mathrm{b}/\Gamma_\mathrm{h}$, $R_\mathrm{c} = \Gamma_\mathrm{c}/\Gamma_\mathrm{h}$, and Γ_T using the given correlation matrices. The data in the upper left-hand column (using $\bar{s}^2_\mathrm{W}(\mathrm{LEP})$ if not otherwise specified) will be referred to as "leptonic sector" in the fits. Inclusion of the data in the upper right-hand column will be referred to as fitting "all data". The theoretical predictions are based on the input parameters [1, 2, 8] given in the lower left-hand column of the table.

analysis reveals that the results for m_t and M_H are independent of the precise value of m_b for any reasonable changes of m_b. Otherwise, the notation in Tab. 1 is standard. The partial Z-boson width into a lepton and an anti-lepton, assuming universality, is denoted by Γ_l. The partial widths for $\mathrm{Z} \to \mathrm{b}\bar{\mathrm{b}}$ and $\mathrm{Z} \to \mathrm{c}\bar{\mathrm{c}}$ are given by Γ_b and Γ_c. Finally, the effective electroweak angle, $\bar{s}^2_\mathrm{W}$, in Tab. 1 is defined by the effective vector and axial vector couplings ($g_\mathrm{V,l}$ and $g_\mathrm{A,l}$, respectively) of the Z boson to leptons at the Z resonance, $\bar{s}^2_\mathrm{W} \equiv \sin^2\theta^\mathrm{lept}_\mathrm{eff} \equiv (1 - g_\mathrm{V,l}/g_\mathrm{A,l})/4$. It is accordingly extracted from the asymmetry measurements at LEP [2] and SLD [3].

The theoretical SM results at the one-loop level, taking into account leading two-loop contributions, are taken from Refs. [9, 10][1]. Therefore, we provide an analysis which is completely independent of results presented by other authors [5, 6, 7].

[1] We have supplemented the analytical results given in Refs. [9, 10] by the $\mathcal{O}(G_\mu m_\mathrm{t}^2 \alpha_\mathrm{s}^2)$ corrections [11] to the ρ-parameter.

We obtain for the global fit to the complete set of data listed in Tab. 1

$$\begin{aligned} m_{\rm t} &= 167^{+11}_{-9}\,\text{GeV}, & M_{\rm H} &= 81^{+144}_{-52}\,\text{GeV}, \\ \alpha(M_{\rm Z}^2)^{-1} &= 128.90 \pm 0.09, & \alpha_{\rm s}(M_{\rm Z}^2) &= 0.121 \pm 0.004, \quad \chi^2_{\rm min}/_{\rm d.o.f.} = 17/9, \end{aligned} \tag{1}$$

where the combined value $\bar{s}^2_{\rm W}(\text{LEP} + \text{SLD})$ has been used. In this fit $\alpha_{\rm s}(M_{\rm Z}^2)$ has been used as a free fit parameter, while the experimental constraints on $\alpha(M_{\rm Z}^2)$ and $m_{\rm t}$ have been included. The result (1) is in good agreement with the corresponding results given in Refs. [6, 7].[2] While the low central value and the rather tight 1σ bounds obtained for $M_{\rm H}$ in this fit seem to indicate evidence for a light Higgs-boson mass, the high value of $\chi^2_{\rm min}/_{\rm d.o.f.} = 17/9$ gives rise to the question of how reliable this bound actually is.

In order to investigate the dependence of the fit results on inclusion/exclusion of different parts of the experimental data, we now turn to an analysis in distinct steps as outlined above. The results for the corresponding fits of the parameters $(m_{\rm t}, M_{\rm H}, \alpha(M_{\rm Z}^2), \alpha_{\rm s}(M_{\rm Z}^2))$ within the SM are presented in Tab. 2 and in the $(M_{\rm H}, \Delta\chi^2)$-plots of Fig. 1. In these fits $\alpha_{\rm s}(M_{\rm Z}^2)$ is treated as a free fit parameter while $\alpha(M_{\rm Z}^2)$ is fitted including the experimental constraint from Tab. 1. Note that the values obtained for $\alpha_{\rm s}(M_{\rm Z}^2)$ in these fits practically coincide with the value of Tab. 1 which is deduced by the entirely different method of an event-shape (jet production) analysis. As mentioned above, $m_{\rm t}$ is treated in two different ways in the fits. Treating $m_{\rm t}$ as a free fit parameter allows to compare its fit result with its actual experimental value, while using this information in the fit from the start leads to a certain "compromise" result which might be more difficult to interpret.

In Fig. 2 we furthermore investigate the dependence of the fit results on variations in $\alpha(M_{\rm Z}^2)$ and $\alpha_{\rm s}(M_{\rm Z}^2)$. To this end these parameters are not fitted but kept as fixed values which are varied within the 1σ bounds of their experimental values given in Tab. 1. The top-quark mass is treated as a free fit parameter in this figure. In the last row of Fig. 2 the effect of replacing $\bar{s}^2_{\rm W}(\text{LEP})$ by $\bar{s}^2_{\rm W}(\text{LEP} + \text{SLD})$ and by $\bar{s}^2_{\rm W}(\text{SLD})$ is studied.

We first of all concentrate on the results of *the first step of our analysis*, namely the fits in Tab. 2a and Fig. 2 based on the data sets $\bar{s}^2_{\rm W}(\text{LEP})$, $\Gamma_{\rm l}$ and $M_{\rm W}$ ("leptonic sector") and $\bar{s}^2_{\rm W}(\text{LEP})$, $\Gamma_{\rm l}$, $M_{\rm W}$, $\Gamma_{\rm T}$, $\Gamma_{\rm h}$ ("all data $\setminus$ $R_{\rm b}, R_{\rm c}$"). Both fits yield an excellent $\chi^2_{\rm min}/_{\rm d.o.f.} < 1$, independently of whether $\alpha(M_{\rm Z}^2)$ and $\alpha_{\rm s}(M_{\rm Z}^2)$ are fitted or whether they are taken as fixed input parameters that are varied within one standard deviation according to Tab. 1. Figure 2 shows that the results of the fits are strongly affected by variations of $\alpha(M_{\rm Z}^2)^{-1}$. For instance, lowering $\alpha(M_{\rm Z}^2)^{-1} = 128.89$ by one standard deviation to $\alpha(M_{\rm Z}^2)^{-1} = 128.80$ also lowers the central value of $M_{\rm H}$ by approximately one standard deviation. Varying $\alpha_{\rm s}(M_{\rm Z}^2)$ from $\alpha_{\rm s}(M_{\rm Z}^2) = 0.123$ to $\alpha_{\rm s}(M_{\rm Z}^2) = 0.117$ shifts the upper 1σ limit of $M_{\rm H}$ from $\sim 1\,\text{TeV}$ to $265\,\text{GeV}$ in the fit in which $\Gamma_{\rm h}$ and $\Gamma_{\rm T}$ are included (second column of Fig. 2). We also note the somewhat low values of the top-quark mass of $m_{\rm t} = 157\,\text{GeV}$ and $m_{\rm t} = 162\,\text{GeV}$ obtained for the lower values of $\alpha(M_{\rm Z}^2)^{-1}$ and $\alpha_{\rm s}(M_{\rm Z}^2)$, respectively, which are below the 1σ lower limit of $m_{\rm t} = 168\,\text{GeV}$ from the direct measurement of $m_{\rm t}$. The fit results in the leptonic sector are stable under variation in the strong coupling constant, $\alpha_{\rm s}(M_{\rm Z}^2)$, since $\alpha_{\rm s}(M_{\rm Z}^2)$ only enters at the two-loop level.

[2] In Ref. [6] also the available low-energy data were included in the analysis, which shows that the effect of these data on the results of the SM fits is rather small.

Table 2a:

using $\bar{s}^2_{\mathrm{W}}$**(LEP)**	$m_{\mathrm{t}}/$ GeV	$M_{\mathrm{H}}/$ GeV	$\alpha_{\mathrm{s}}(M_{\mathrm{Z}}^2)$	$\chi^2_{\mathrm{min}}/_{\mathrm{d.o.f.}}$
leptonic sector $+ m_{\mathrm{t}}^{\mathrm{exp}}$	179^{+12}_{-11}	353^{+540}_{-224}	0.123 (fixed)	0.2/5
leptonic sector	174^{+37}_{-19}	$248^{+\gtrsim 1000}_{-194}$	0.123 (fixed)	0.2/4
all data $+ m_{\mathrm{t}}^{\mathrm{exp}} \setminus R_{\mathrm{b}}, R_{\mathrm{c}}$	179^{+12}_{-12}	356^{+543}_{-227}	$0.124^{+0.004}_{-0.004}$	0.7/7
all data $\setminus R_{\mathrm{b}}, R_{\mathrm{c}}$	167^{+45}_{-20}	$163^{+\gtrsim 1000}_{-126}$	$0.123^{+0.007}_{-0.004}$	0.6/6
all data $+ m_{\mathrm{t}}^{\mathrm{exp}} \setminus R_{\mathrm{b}}$	178^{+12}_{-12}	343^{+523}_{-219}	$0.124^{+0.004}_{-0.004}$	6.6/8
all data $\setminus R_{\mathrm{b}}$	164^{+40}_{-18}	$133^{+\gtrsim 1000}_{-97}$	$0.123^{+0.006}_{-0.004}$	6.4/7
all data $+ m_{\mathrm{t}}^{\mathrm{exp}} \setminus R_{\mathrm{c}}$	169^{+11}_{-11}	186^{+277}_{-119}	$0.123^{+0.004}_{-0.004}$	15/8
all data $\setminus R_{\mathrm{c}}$	148^{+14}_{-12}	54^{+93}_{-30}	$0.122^{+0.004}_{-0.004}$	12/7
all data $+ m_{\mathrm{t}}^{\mathrm{exp}}$	170^{+11}_{-11}	197^{+291}_{-126}	$0.123^{+0.004}_{-0.004}$	16/9
all data	149^{+15}_{-12}	57^{+104}_{-32}	$0.122^{+0.004}_{-0.004}$	14/8

Table 2b:

using $\bar{s}^2_{\mathrm{W}}$**(LEP + SLD)**	$m_{\mathrm{t}}/$ GeV	$M_{\mathrm{H}}/$ GeV	$\alpha_{\mathrm{s}}(M_{\mathrm{Z}}^2)$	$\chi^2_{\mathrm{min}}/_{\mathrm{d.o.f.}}$
leptonic sector $+ m_{\mathrm{t}}^{\mathrm{exp}}$	175^{+12}_{-11}	152^{+282}_{-106}	0.123 (fixed)	1.0/5
leptonic sector	165^{+18}_{-10}	64^{+223}_{-37}	0.123 (fixed)	0.3/4
all data $+ m_{\mathrm{t}}^{\mathrm{exp}} \setminus R_{\mathrm{b}}, R_{\mathrm{c}}$	176^{+12}_{-12}	154^{+273}_{-108}	$0.122^{+0.004}_{-0.004}$	1.5/7
all data $\setminus R_{\mathrm{b}}, R_{\mathrm{c}}$	161^{+21}_{-12}	51^{+214}_{-31}	$0.121^{+0.007}_{-0.004}$	0.7/6
all data $+ m_{\mathrm{t}}^{\mathrm{exp}} \setminus R_{\mathrm{b}}$	175^{+12}_{-11}	148^{+263}_{-103}	$0.122^{+0.004}_{-0.004}$	7.3/8
all data $\setminus R_{\mathrm{b}}$	160^{+19}_{-12}	49^{+174}_{-29}	$0.121^{+0.004}_{-0.004}$	6.5/7
all data $+ m_{\mathrm{t}}^{\mathrm{exp}} \setminus R_{\mathrm{c}}$	167^{+11}_{-9}	76^{+136}_{-49}	$0.121^{+0.004}_{-0.004}$	15/8
all data $\setminus R_{\mathrm{c}}$	152^{+11}_{-11}	34^{+46}_{-17}	$0.122^{+0.004}_{-0.004}$	12/7
all data $+ m_{\mathrm{t}}^{\mathrm{exp}}$	167^{+11}_{-9}	81^{+144}_{-52}	$0.121^{+0.004}_{-0.004}$	17/9
all data	153^{+11}_{-11}	35^{+50}_{-18}	$0.121^{+0.004}_{-0.004}$	14/8

Table 2: The results obtained in $(m_{\mathrm{t}}, M_{\mathrm{H}}, \alpha(M_{\mathrm{Z}}^2), \alpha_{\mathrm{s}}(M_{\mathrm{Z}}^2))$ fits to different sets of experimental data, as indicated (see text). The results in Tab. 2a are based on $\bar{s}^2_{\mathrm{W}}(\mathrm{LEP})$, while the results in Tab. 2b are based on $\bar{s}^2_{\mathrm{W}}(\mathrm{LEP}+\mathrm{SLD})$. For each set of experimental data, the fit results given in the lower row are obtained by treating m_{t} as a free fit parameter, while the results in the upper row include the constraint $m_{\mathrm{t}}^{\mathrm{exp}} = 180 \pm 12\,\mathrm{GeV}$. Note that the fit results on $\alpha(M_{\mathrm{Z}}^2)$ are not explicitly stated, because they range between $\alpha(M_{\mathrm{Z}}^2)^{-1} = 128.89 \pm 0.09$ and $\alpha(M_{\mathrm{Z}}^2)^{-1} = 128.91 \pm 0.09$ for all cases, thus reproducing the input value from Tab. 1.

$m_{\rm t}$/ GeV fixed	144	168	180	192
	$M_{\rm H}$/ GeV ($\chi^2_{\rm min}/_{\rm d.o.f.}$)			
leptonic sector	47^{+30}_{-18} (4.2/3)	160^{+104}_{-69} (0.2/3)	362^{+206}_{-136} (0.2/3)	792^{+444}_{-280} (0.4/3)
all data \ $R_{\rm b}$, $R_{\rm c}$	44^{+34}_{-20} (2.1/5)	172^{+110}_{-73} (0.6/5)	349^{+196}_{-131} (0.8/5)	682^{+368}_{-239} (1.3/5)
all data \ $R_{\rm b}$	44^{+34}_{-20} (7.7/6)	174^{+111}_{-73} (6.4/6)	353^{+199}_{-133} (6.7/6)	689^{+375}_{-242} (7.3/6)
all data \ $R_{\rm c}$	45^{+35}_{-21} (12/6)	176^{+112}_{-74} (14/6)	355^{+199}_{-133} (16/6)	685^{+368}_{-239} (19/6)
all data	45^{+35}_{-21} (14/7)	176^{+112}_{-74} (15/7)	355^{+199}_{-133} (17/7)	686^{+369}_{-240} (20/7)

Table 3: Fits of $M_{\rm H}$ to various sets of experimental data in the SM for fixed values of $m_{\rm t}$. In all fits $\alpha(M_{\rm Z}^2)^{-1} = 128.89$ and $\alpha_{\rm s}(M_{\rm Z}^2) = 0.123$ are kept fixed, and the LEP value of $\bar{s}^2_{\rm W}$ is used in the input data.

Altogether, we thus conclude that varying $\alpha(M_{\rm Z}^2)^{-1}$ and $\alpha_{\rm s}(M_{\rm Z}^2)$ within the 1σ bounds given in Tab. 1 leads to a considerable effect concerning the boundaries in the $(m_{\rm t}, M_{\rm H})$ plane. Consequently, concerning the range of $M_{\rm H}$ allowed by the results from the leptonic sector (with $\bar{s}^2_{\rm W}$(LEP)) and $\Gamma_{\rm T}, \Gamma_{\rm h}$, i.e. by fitting the SM only to those data that agree with the theoretical predictions, according to the foregoing discussion of Tab. 2a and Fig. 2, it seems hardly possible to deduce stronger limits than $M_{\rm H} \lesssim 900\,{\rm GeV}$ at the 1σ level, even upon taking into account the constraint of $m_{\rm t}^{\rm exp} = 180 \pm 12\,{\rm GeV}$ from the direct observation of the top quark.

We turn to the *second step of our analysis* and include $R_{\rm b}$ in the fit, which is thus based on the leptonic sector in conjunction with $\Gamma_{\rm T}$, $\Gamma_{\rm h}$ and $R_{\rm b}$. According to Tab. 2a and Fig. 2, taking into account the data for the ${\rm Z} \to {\rm b\bar{b}}$ partial width leads to an increase of $\chi^2_{\rm min}/_{\rm d.o.f.}$ by about an order of magnitude. Comparing the third column in Fig. 2 with the first and second columns, one observes a considerable shrinkage of the 1σ regions in the $(m_{\rm t}, M_{\rm H})$ plane and a drastic shift towards lower values of $m_{\rm t}$ and $M_{\rm H}$. The sensitivity against variations of $\alpha(M_{\rm Z}^2)^{-1}$ and $\alpha_{\rm s}(M_{\rm Z}^2)$ is considerably weaker in this sample of data. The central fit-value for the top-quark mass of $m_{\rm t} = 148^{+14}_{-12}\,{\rm GeV}$ (where the experimental constraint on $m_{\rm t}$ has not been taken into account in the fit) is significantly below the central value of the direct measurement of $m_{\rm t}^{\rm exp} = 180 \pm 12\,{\rm GeV}$, and the central value obtained for the Higgs-boson mass, $M_{\rm H} = 54^{+93}_{-30}\,{\rm GeV}$, lies in the vicinity of the experimental lower bound $M_{\rm H} > 65.2\,{\rm GeV}$.

The large increase of $\chi^2_{\rm min}/_{\rm d.o.f.}$ when including $R_{\rm b}$ in the fit signals the large discrepancy between theory and experiment in this fit. In particular, when evaluating $R_{\rm b}$ for the best-fit values of $(m_{\rm t}, M_{\rm H}) = (148^{+14}_{-12}\,{\rm GeV}, 54^{+93}_{-30}\,{\rm GeV})$, the resulting ($M_{\rm H}$-insensitive) theoretical prediction, $R_{\rm b}^{\rm SM} = 0.2164^{-0.0005}_{+0.0004}$ (with the errors indicating the changes by varying $m_{\rm t}$ within the 1σ limits), still lies more than 3σ below the experimental value of $R_{\rm b} = 0.2219 \pm 0.0017$.

In connection with the low central fit value of $m_{\rm t} = 148\,{\rm GeV}$, it is illuminating to consider the results of single-parameter $M_{\rm H}$ fits, where $m_{\rm t}$ is kept fixed at certain (assumed)

values. In Tab. 3, again for the previously selected sets of data, results of single-parameter M_{H} fits are shown. The known strong $(m_{\mathrm{t}}, M_{\mathrm{H}})$ correlation in SM fits leads to a remarkable stability of the resulting fit values for M_{H}. Once m_{t} is fixed, there is almost no dependence of the fit value for M_{H} on which set of input data is actually used in the fit. In particular, whenever a low value of m_{t} is chosen, one obtains a low value for M_{H}, independently of whether R_{b} is included in the fit or not.[3] Since the (M_{H}-insensitive) SM prediction for R_{b} increases with decreasing m_{t}, in the combined fit of $(m_{\mathrm{t}}, M_{\mathrm{H}})$ the inclusion of R_{b} lowers the fit value of m_{t}, and via the $(m_{\mathrm{t}}, M_{\mathrm{H}})$ correlation also the value of M_{H}. As discussed above, the result of $m_{\mathrm{t}} = 148\,\mathrm{GeV}$ is nothing but a kind of compromise, as it still leads to a 3σ discrepancy between theory and experiment in R_{b}. Moreover, this result for m_{t} is disfavored by the Tevatron result of $m_{\mathrm{t}}^{\mathrm{exp}} = 180 \pm 12\,\mathrm{GeV}$.

While the problematic features of the fits where R_{b} is included are easy to see in the case where m_{t} is used as a free fit parameter, they are somewhat hidden in the fits where the experimental information on m_{t} is used. It partially compensates the tendency of the fits towards low values of m_{t} and leads to the more moderate looking result of $m_{\mathrm{t}} = 169 \pm 11\,\mathrm{GeV}$ and $M_{\mathrm{H}} = 186^{+277}_{-119}\,\mathrm{GeV}$. In view of the foregoing discussion, however, the result for M_{H} obtained in this way appears to be rather questionable.

In summary, the large value of $\chi^2_{\mathrm{min}}/_{\mathrm{d.o.f.}}$ and the low fit value for m_{t} (when m_{t} is treated as free fit parameter) that is at variance with the Tevatron result, lead to the conclusion that the low value and tight bound obtained for M_{H} when including the data for R_{b} does not seem reliable. It is an artifact of the procedure of describing the "non-standard" value of R_{b} by the unmodified SM in conjunction with the $(m_{\mathrm{t}}, M_{\mathrm{H}})$ correlation. This conclusion is strengthened by the fact that a simple phenomenological modification of the $\mathrm{Z} \to \mathrm{b}\bar{\mathrm{b}}$ vertex, to be discussed below, leads to values of m_{t} compatible with the Tevatron result and removes the stringent upper bounds on M_{H}.

We turn to the third step of our analysis and consider the *impact of the observable* R_{c}. As can be seen in Tab. 2, the results for m_{t} and M_{H} are hardly affected by including R_{c}. This is a consequence of the fact that the contribution of R_{c} to χ^2 depends only very weakly on m_{t} and M_{H}, because the experimental error for R_{c} is much larger than the change in the SM prediction for R_{c} induced by varying m_{t} and M_{H}. Similarly to the case of R_{b}, including R_{c} in the set of data (and omitting R_{b}) leads to an enhanced value of $\chi^2_{\mathrm{min}}/_{\mathrm{d.o.f.}}$ and to a tendency towards lower values of M_{H}.

So far the analysis has been based on the LEP experimental value of $\bar{s}^2_{\mathrm{W}}(\mathrm{LEP})$. Table 2b and the last row of Fig. 2 show the *effect of replacing* $\bar{s}^2_{\mathrm{W}}(\mathrm{LEP})$ *by* $\bar{s}^2_{\mathrm{W}}(\mathrm{LEP}+\mathrm{SLD})$. In Fig. 2 also contours are shown that are based on taking $\bar{s}^2_{\mathrm{W}}(\mathrm{SLD})$ alone. The change in the allowed $(m_{\mathrm{t}}, M_{\mathrm{H}})$ plane occurring as a consequence of these replacements is very strong. For the "leptonic sector" and "all data $\setminus$ $R_{\mathrm{b}}, R_{\mathrm{c}}$" the fit value of $m_{\mathrm{t}} \simeq 170\,\mathrm{GeV}$ (where $m_{\mathrm{t}}^{\mathrm{exp}}$ has not been included in the fit) is consistent with the value from the direct measurements, $m_{\mathrm{t}}^{\mathrm{exp}} = 180 \pm 12\,\mathrm{GeV}$, while the values for M_{H} resulting from using $\bar{s}^2_{\mathrm{W}}(\mathrm{SLD})$ now have decreased to $M_{\mathrm{H}} = 18^{+28}_{-9}\,\mathrm{GeV}$ and $M_{\mathrm{H}} = 16^{+27}_{-9}\,\mathrm{GeV}$, respectively. The fit to "all data" using $\bar{s}^2_{\mathrm{W}}(\mathrm{SLD})$ yields $m_{\mathrm{t}} = 161^{+10}_{-11}\,\mathrm{GeV}$ and a similarly low value for M_{H}, namely

[3] Conversely, if M_{H} is fixed, the values of m_{t} obtained in the fit are fairly stable, independently of whether R_{b} or R_{c} are included in the fit or not. This is consistent with the results of Ref. [2], where $M_{\mathrm{H}} = 300\,\mathrm{GeV}$ is kept fixed when fitting m_{t}.

$M_{\mathrm{H}} = 18^{+24}_{-9}\,\mathrm{GeV}$. Accordingly, using the SLD value for $\bar{s}^2_{\mathrm{W}}$ leads to very low fit results for M_{H}, independently of whether R_{b} and R_{c} are included in the data set or not, and of whether use is made of the experimental information on m_{t}. Comparing these results to the lower bound from the direct Higgs-boson search, $M_{\mathrm{H}} > 65.2\,\mathrm{GeV}$ [12], one arrives at a serious conflict between the unmodified SM and experiment. The discrepancy is weakened if the combined value of $\bar{s}^2_{\mathrm{W}}(\mathrm{LEP}+\mathrm{SLD})$ from Tab. 2b is used. In this case one obtains $m_{\mathrm{t}} = 153 \pm 11\,\mathrm{GeV}$ and $M_{\mathrm{H}} = 35^{+50}_{-18}\,\mathrm{GeV}$ for "all data" (where again $m_{\mathrm{t}}^{\mathrm{exp}}$ has not been included). A resolution of the LEP–SLD discrepancy on $\bar{s}^2_{\mathrm{W}}$ is obviously one of the most important tasks with respect to the issue of M_{H} bounds via radiative corrections.

As a summary of the present situation concerning M_{H}, in Fig. 1 we present the result of selected $(m_{\mathrm{t}}, M_{\mathrm{H}}, \alpha(M_{\mathrm{Z}}^2), \alpha_{\mathrm{s}}(M_{\mathrm{Z}}^2))$ fits according to Tab. 2 in a $(M_{\mathrm{H}}, \Delta\chi^2)$ plot. The quantitative influence on the fit value of M_{H} resulting from inclusion of $m_{\mathrm{t}}^{\mathrm{exp}} = 180 \pm 12\,\mathrm{GeV}$ can be seen to agree with the qualitative expectations from Fig. 2. Other features of the results for M_{H} previously read off from Fig. 2, such as the correlation between M_{H} and the input for $\bar{s}^2_{\mathrm{W}}$, or the effect of ignoring the experimental results for R_{b}, R_{c} can obviously also be seen in Fig. 1. The plots in Fig. 1 clearly illustrate the difficulty of establishing a unique bound on M_{H}. The most reliable bound, from "all data $\setminus R_{\mathrm{b}}, R_{\mathrm{c}}$", but including $m_{\mathrm{t}}^{\mathrm{exp}}$ yields $M_{\mathrm{H}} \lesssim 430\,\mathrm{GeV}$ based on $\bar{s}^2_{\mathrm{W}}(\mathrm{LEP}+\mathrm{SLD})$, and $M_{\mathrm{H}} \lesssim 900\,\mathrm{GeV}$ based on $\bar{s}^2_{\mathrm{W}}(\mathrm{LEP})$.

In order to accommodate the experimental result for R_{b}, we now allow for a *modification of the* $\mathrm{Z} \to \mathrm{b}\bar{\mathrm{b}}$ *vertex* by a parameter Δy_{b}, as introduced in Ref. [10].[4] The possible origin of this modification of the SM predictions is left open for the time being, but in particular it includes the impact of new particles in conjunction with loop corrections at the $\mathrm{Z} \to \mathrm{b}\bar{\mathrm{b}}$ vertex. We allow for values of $\alpha_{\mathrm{s}}(M_{\mathrm{Z}}^2)$ different [14] from the LEP value of $\alpha_{\mathrm{s}}(M_{\mathrm{Z}}^2) = 0.123$, in order to compensate for the enhanced theoretical value of the total hadronic Z-boson width, Γ_{h}, resulting from the enlarged theoretical value of Γ_{b} which is adjusted to be in agreement with experiment. Deviations of Δy_{b} from its (m_{t}-dependent) SM value $\Delta y_{\mathrm{b}}^{\mathrm{SM}}$ [10] lead to an extra contribution X_{b} [2] in the prediction for Γ_{b},

$$\begin{aligned} X_{\mathrm{b}} = \Gamma_{\mathrm{b}} - \Gamma_{\mathrm{b}}^{\mathrm{SM}} &= \frac{\alpha(M_{\mathrm{Z}}^2) M_{\mathrm{Z}}}{24 s_0^2 c_0^2} (2 s_0^2 - 3)\, R_{\mathrm{QED}}\, R_{\mathrm{QCD}} \left(\Delta y_{\mathrm{b}} - \Delta y_{\mathrm{b}}^{\mathrm{SM}}\right) \\ &= -0.421\,\mathrm{GeV} \times R_{\mathrm{QCD}} \left(\Delta y_{\mathrm{b}} - \Delta y_{\mathrm{b}}^{\mathrm{SM}}\right), \end{aligned} \tag{2}$$

where $s_0^2 c_0^2 = s_0^2(1 - s_0^2) = \pi\alpha(M_{\mathrm{Z}}^2)/\sqrt{2} G_\mu M_{\mathrm{Z}}^2$, $R_{\mathrm{QED}} = 1 + \alpha/12\pi$, and $R_{\mathrm{QCD}} = 1 + \alpha_{\mathrm{s}}(M_{\mathrm{Z}}^2)/\pi + 1.41(\alpha_{\mathrm{s}}(M_{\mathrm{Z}}^2)/\pi)^2 - 12.8(\alpha_{\mathrm{s}}(M_{\mathrm{Z}}^2)/\pi)^3$ according to Ref. [15].

In Tab. 4 we present our results for four-parameter $(m_{\mathrm{t}}, M_{\mathrm{H}}, \Delta y_{\mathrm{b}}, \alpha(M_{\mathrm{Z}}^2))$ fits with fixed values of $\alpha_{\mathrm{s}}(M_{\mathrm{Z}}^2)$, as well as the results of five-parameter $(m_{\mathrm{t}}, M_{\mathrm{H}}, \Delta y_{\mathrm{b}}, \alpha(M_{\mathrm{Z}}^2), \alpha_{\mathrm{s}}(M_{\mathrm{Z}}^2))$ fits. Table 4a is based on the data set "all data $+\, m_{\mathrm{t}}^{\mathrm{exp}} \setminus R_{\mathrm{c}}$" (experimental information on m_{t} included), while in Tab. 4b we have used "all data $\setminus R_{\mathrm{c}}$" (m_{t} treated as a free fit parameter). The conclusion from Tab. 4 is simple: once one allows for a modification of R_{b} by the parameter Δy_{b}, the bounds on M_{H} obtained by fitting within the unmodified SM are lost. The quality of the fit is improved considerably, if one allows for a value

[4] The parameter Δy_{b} is related to the parameter ε_{b} introduced in Ref. [13] via $\Delta y_{\mathrm{b}} = -2\varepsilon_{\mathrm{b}} - 0.2 \times 10^{-3}$ (see Ref. [10]).

Table 4a (“all data $+m_t^{exp} \setminus R_c$”):

$\alpha_s(M_Z^2)$	m_t/ GeV	M_H/ GeV	$\Delta y_b/10^{-3}$	$\chi^2_{min}/_{d.o.f.}$
0.123 fixed	179^{+11}_{-11}	$582^{+\gtrsim 1000}_{-324}$	$3.9^{+4.6}_{-4.6}$	11/8
0.110 fixed	179^{+11}_{-11}	$523^{+\gtrsim 1000}_{-302}$	$-8.8^{+4.6}_{-4.6}$	3.4/8
0.100 fixed	179^{+12}_{-11}	$472^{+\gtrsim 1000}_{-284}$	$-18.6^{+4.6}_{-4.6}$	0.9/8
0.098 ± 0.008 fitted	179^{+12}_{-12}	$459^{+\gtrsim 1000}_{-281}$	$-20.9^{+8.9}_{-8.9}$	0.9/8

Table 4b (“all data $\setminus R_c$”):

$\alpha_s(M_Z^2)$	m_t/ GeV	M_H/ GeV	$\Delta y_b/10^{-3}$	$\chi^2_{min}/_{d.o.f.}$
0.123 fixed	173^{+28}_{-22}	$414^{+\gtrsim 1000}_{-294}$	$3.8^{+4.6}_{-4.6}$	11/7
0.110 fixed	174^{+32}_{-23}	$375^{+\gtrsim 1000}_{-284}$	$-8.8^{+4.6}_{-4.6}$	3.3/7
0.100 fixed	172^{+37}_{-24}	$300^{+\gtrsim 1000}_{-236}$	$-18.6^{+4.7}_{-4.6}$	0.9/7
0.098 ± 0.008 fitted	171^{+39}_{-24}	$269^{+\gtrsim 1000}_{-216}$	$-21.0^{+8.9}_{-9.0}$	0.8/7

Table 4: The results of four-parameter and five-parameter fits to “all data $\setminus R_c$” with m_t^{exp} in-/excluded. In the four-parameter $(m_t, M_H, \Delta y_b, \alpha(M_Z^2))$ fits $\alpha_s(M_Z^2)$ is kept fixed as indicated (first three rows), while in the five-parameter $(m_t, M_H, \Delta y_b, \alpha(M_Z^2), \alpha_s(M_Z^2))$ fits (last row) $\alpha_s(M_Z^2)$ is treated as a free fit parameter. The fit results for $\alpha(M_Z^2)$ are again omitted, since they merely vary between $\alpha(M_Z^2)^{-1} = 128.90 \pm 0.09$ and $\alpha(M_Z^2)^{-1} = 128.92 \pm 0.09$.

of $\alpha_s(M_Z^2)$ substantially below the LEP result from the event shape measurement [2] of $\alpha_s(M_Z^2) = 0.123 \pm 0.006$. Fitting also $\alpha_s(M_Z^2)$ leads to the extremely low best-fit value of $\alpha_s(M_Z^2) = 0.098 \pm 0.008$, which is even lower than the extrapolated value of $\alpha_s(M_Z^2)$ from low-energy deep inelastic scattering data, $\alpha_s(M_Z^2) = 0.112 \pm 0.004$ [15], and the value obtained from lattice QCD calculations, $\alpha_s(M_Z^2) = 0.115 \pm 0.003$ [15]. The values of m_t in Tab. 4b roughly coincide with the ones obtained in the SM fits to the “leptonic sector” given in Tab. 2a. For low $\alpha_s(M_Z^2)$ also the M_H bounds in Tab. 4b are similar to the results of the SM fit obtained for the “leptonic sector” (Tab. 2a).

As in the previous case of the pure SM fits, the results do not change qualitatively when R_c is included in the data set. In the $(m_t, M_H, \Delta y_b, \alpha(M_Z^2), \alpha_s(M_Z^2))$ fit to “all data $+m_t^{exp}$” we obtain

$$m_t = 179 \pm 12\,\mathrm{GeV}, \qquad \mathrm{M_H} = 440^{+\gtrsim 1000}_{-270}\,\mathrm{GeV}, \qquad \alpha(\mathrm{M_Z^2})^{-1} = 128.90 \pm 0.09,$$
$$\alpha_s(M_Z^2) = 0.102 \pm 0.008, \qquad \Delta y_b = (\,-15.2^{+8.5}_{-8.6}\,) \times 10^{-3}, \qquad \chi^2_{min}/_{d.o.f.} = 5.8/9. \tag{3}$$

This is in good agreement with the results presented in Ref. [2] for a fit of (m_t, α_s, X_b) for M_H fixed at $M_H = 300\,\mathrm{GeV}$. The increased value of $\chi^2_{min}/_{d.o.f.}$ in (3) relative to the corresponding value in Tab. 4 is of course a consequence of the 2.5σ discrepancy [2] in R_c. However, it does not seem to be meaningful to introduce an additional non-

$\alpha_s(M_Z^2)$	0.123	0.099	0.123	0.099
$\chi^2_{\min}/_{\text{d.o.f.}}$	0		9.3/6	0.5/6
$\Delta x^{\exp}/10^{-3}$	10.1 ± 4.2		9.9 ± 4.2	10.1 ± 4.2
$\Delta y^{\exp}/10^{-3}$	5.4 ± 4.3		7.0 ± 4.3	5.7 ± 4.3
$\varepsilon^{\exp}/10^{-3}$	-5.3 ± 1.6		-4.2 ± 1.5	-5.0 ± 1.5
$\Delta y_b^{\exp}/10^{-3}$	-14.6 ± 6.9	-20.9 ± 7.0	0.7 ± 4.7	-20.5 ± 4.7
$\Delta y_h^{\exp}/10^{-3}$	4.9 ± 2.3	-1.7 ± 2.3	-1.4 (from theory)	
$\Delta y_\nu^{\exp}/10^{-3}$	0.6 ± 5.2		-3.0 (from theory)	

Table 5: Experimental results for the effective parameters for $\alpha_s(M_Z^2) = 0.123$ and the low value $\alpha_s(M_Z^2) = 0.099$. The entries on the left-hand side are obtained by determining the six effective parameters from the six observables Γ_l, $\bar{s}_W^2(\text{LEP})$, M_W, Γ_T, Γ_h, and Γ_b. On the right-hand side Δy_h and Δy_ν have been taken from theory, and the remaining parameters have been fitted twice, namely for fixed $\alpha_s(M_Z^2) = 0.123$ and with $\alpha_s(M_Z^2)$ as additional fit parameter, resulting in $\alpha_s(M_Z^2) = 0.099$.

standard parameter Δy_c in order to accommodate the R_c discrepancy. On the one hand, a modification of the $Z \to c\bar{c}$ vertex is much less motivated than in the case of the $Z \to b\bar{b}$ vertex (see e.g. the discussion in Ref. [10]); on the other hand, a fit in which a non-standard Δy_c is allowed yields the absurd value $\alpha_s(M_Z^2) = 0.19 \pm 0.04$, which was also obtained e.g. in Refs. [2, 7, 15].

As a final point, we compare the $(m_t, M_H, \Delta y_b, \alpha(M_Z^2), \alpha_s(M_Z^2))$-fit discussed above with an analysis based on *phenomenological effective parameters*. The six observables Γ_l, $\bar{s}_W^2(\text{LEP})$, M_W and Γ_T, Γ_h, Γ_b can be represented as linear combinations of six phenomenological parameters Δx, Δy, ε and $\Delta y_h = (\Delta y_u + \Delta y_d)/2 + (s_0^2/6c_0^2)(\Delta y_d - \Delta y_u)$, Δy_b, Δy_ν that describe possible sources of SU(2) violation within an effective Lagrangian for electroweak interactions at the Z-boson resonance [10]. We assume that the QCD corrections, such as R_{QCD}, which enter Γ_T, Γ_h, and Γ_b, have standard form. These corrections are extracted from the experimental data before the determination of the effective parameters (see Ref. [10]), which therefore quantify all electroweak corrections to the $\alpha(M_Z^2)$-Born approximation.

The results of extracting the experimental values of the six parameters $\Delta x^{\exp}$ etc. from the six observables by inverting the system of linear equations is shown on the left-hand side of Tab. 5. The α_s-dependence only affects $\Delta y_b^{\exp}$ and $\Delta y_h^{\exp}$, since the leptonic sector by itself determines $\Delta x^{\exp}$, $\Delta y^{\exp}$ and $\varepsilon^{\exp}$. The values of $\Delta x^{\exp}$, $\Delta y^{\exp}$ and $\varepsilon^{\exp}$ are in excellent agreement with their SM predictions, as discussed in detail for the data of Refs. [2, 3] in Ref. [16]. For $\alpha_s(M_Z^2) = 0.123$, in addition to the non-standard value of $\Delta y_b^{\exp}$, also the parameter $\Delta y_h^{\exp}$ disagrees with the theoretical prediction [10] of $\Delta y_h^{\text{SM}} = -3.0 \times 10^{-3}$.

Agreement between SM and experiment in $\Delta y_{\rm h}$ is achieved, however, for low values of $\alpha_{\rm s}(M_{\rm Z}^2)$, such as $\alpha_{\rm s}(M_{\rm Z}^2) = 0.099$.

Noting that the process-specific parameters $\Delta y_{\rm h}$ and Δy_ν only depend [10] on the empirically well-established[5] couplings between vector-bosons and light fermions (i.e. all fermions except for top and bottom quarks), we now impose the SM values for $\Delta y_{\rm h}$ and Δy_ν and determine the remaining parameters in a fit. According to the right-hand side of Tab. 5, for fixed $\alpha_{\rm s}(M_{\rm Z}^2) = 0.123$, we find a rather poor quality of the fit ($\chi^2_{\rm min}/_{\rm d.o.f.} = 9.3/6$). Allowing for $\alpha_{\rm s}(M_{\rm Z}^2)$ as additional fit parameter, we obtain an excellent quality of the fit ($\chi^2_{\rm min}/_{\rm d.o.f.} = 0.5/6$), and for $\alpha_{\rm s}(M_{\rm Z}^2)$ the low value of $\alpha_{\rm s}(M_{\rm Z}^2) = 0.099$ deliberately chosen before.

It has thus been shown that the low value for $\alpha_{\rm s}(M_{\rm Z}^2)$, as a consequence of the experimental value of $R_{\rm b}$, emerges independently of much of the details of electroweak radiative corrections. The two very weak assumptions made here, namely standard form of the QCD corrections and of Δy_ν and $\Delta y_{\rm h}$, already imply the very low value of $\alpha_{\rm s}(M_{\rm Z}^2) = 0.099 \pm 0.008$ in the fit which includes $R_{\rm b}$. This value is very close to the one obtained above in the $(m_{\rm t}, M_{\rm H}, \Delta y_{\rm b}, \alpha(M_{\rm Z}^2), \alpha_{\rm s}(M_{\rm Z}^2))$ fit, where non-standard contributions have only been allowed in the $\rm Z \to b\bar{b}$ vertex. Moreover, the values of $\Delta y_{\rm b} = 0.7 \pm 4.7$ for $\alpha_{\rm s}(M_{\rm Z}^2) = 0.123$ and of $\Delta y_{\rm b} = -20.5 \pm 4.7$ for $\alpha_{\rm s}(M_{\rm Z}^2) = 0.099$ (as well as $\Delta x^{\rm exp}$, $\Delta y^{\rm exp}$, $\varepsilon^{\rm exp}$) obtained in the present analysis are in good agreement with the values given in Tab. 4 for the $(m_{\rm t}, M_{\rm H}, \Delta y_{\rm b}, \alpha(M_{\rm Z}^2))$ fit. In both treatments a decent value of $\chi^2_{\rm min}/_{\rm d.o.f.}$ therefore requires a value of $\alpha_{\rm s}(M_{\rm Z}^2)$ that, in the best-fit case, is four standard deviations below $\alpha_{\rm s}(M_{\rm Z}^2) = 0.123 \pm 0.006$.

In summary, from our analysis of the precision data at the Z-boson resonance and $M_{\rm W}$, we find that a Higgs-boson mass lying in the perturbative regime of the Standard Model, i.e. below 1 TeV, is indeed favored at the 1σ level. Having investigated in much detail the impact of the data for the $\rm Z \to b\bar{b}, c\bar{c}$ decay modes and the experimental value of $\bar{s}^2_{\rm W}(\rm SLD)$, as well as the influence of the uncertainties connected with the input parameters $\alpha(M_{\rm Z}^2)$ and $\alpha_{\rm s}(M_{\rm Z}^2)$, we conclude that a stronger upper 1σ bound on $M_{\rm H}$ than $M_{\rm H} \lesssim 900\,\rm GeV$ based on $\bar{s}^2_{\rm W}(\rm LEP)$ and $M_{\rm H} \lesssim 430\,\rm GeV$ based on $\bar{s}^2_{\rm W}(\rm LEP + SLD)$ can hardly be justified from the data at present. The stringent bounds on $M_{\rm H}$ that are obtained when the unmodified Standard Model is fitted to the complete data sample are immediately lost when $R_{\rm b}$ and $\bar{s}^2_{\rm W}(\rm SLD)$ are excluded from the analysis or, as demonstrated for the case of $R_{\rm b}$, if non-standard contributions are allowed in the theoretical model. The well-known fact that allowing for a non-standard contribution to $R_{\rm b}$ gives rise to an extremely low value of $\alpha_{\rm s}(M_{\rm Z}^2)$ has been shown to emerge already under the weak theoretical assumptions of standard QCD corrections and standard form of the couplings of the gauge-bosons to the leptons and to the quarks of the first two generations.

Note added in proof: The most recent value from the Tevatron on $m_{\rm t}$ is given by $m_{\rm t}^{\rm exp} = 175 \pm 9\,\rm GeV$. All essential conclusions of the present work, based on $m_{\rm t}^{\rm exp} = 180 \pm 12\,\rm GeV$, remain valid if this most recent value of $m_{\rm t}^{\rm exp}$ is used.

[5]Here we ignore the $R_{\rm c}$ problem, previously commented upon.

Acknowledgement

G.W. thanks A. Djouadi for useful discussions.

References

[1] CDF collaboration, F. Abe et al., *Phys. Rev. Lett.* **74** (1995) 2626;
DØ collaboration, S. Abachi et al., *Phys. Rev. Lett.* **74** (1995) 2632.

[2] LEP Collaboration ALEPH, DELPHI, L3, OPAL and the LEP Electroweak Working Group, Data presented at the 1995 Summer Conferences, LEPEWWG/95-02.

[3] SLD Collaboration: K. Abe et al., *Phys. Rev. Lett.* **73** (1994) 25;
SLD Collaboration: K. Abe et al., contributed paper to EPS-HEP-95, Brussels, eps0654.

[4] UA(2) Collaboration: J. Alitti et al., *Phys. Lett.* **B276** (1992) 354;
CDF Collaboration: F. Abe et al., *Phys. Rev. Lett.* **65** (1990) 2243, *Phys. Rev.* **D43** (1991) 2070;
CDF Collaboration: F. Abe et al., *Phys. Rev. Lett.* **75** (1995) 11;
DØ Collaboration: C.K. Jung, Proc. of the XXVII Int. Conf. on High Energy Physics, Glasgow, July 1994, eds. P.J. Bussey and I.G. Knowles.

[5] G. Montagna, O. Nicrosini, G. Passarino and F. Piccinini, *Phys. Lett.* **B335** (1994) 484;
V.A. Novikov, L.B. Okun, A.N. Rozanov and M.I. Vysotskii, *Mod. Phys. Lett.* **A9** (1994) 2641;
J. Erler and P. Langacker, *Phys. Rev.* **D52** (1995) 441;
S. Matsumoto, *Mod. Phys. Lett.* **A10** (1995) 2553;
Z. Hioki, TOKUSHIMA 95-04, hep-ph/9510269;
K. Kang and S.K. Kang, BROWN-HET-979, hep-ph/9503478.

[6] J. Ellis, G.L. Fogli and E. Lisi, CERN-TH/95-202, hep-ph/9507424.

[7] P.H. Chankowski and S. Pokorski, *Phys. Lett.* **B356** (1995) 307; hep-ph/9509207.

[8] H. Burkhardt and B. Pietrzyk, *Phys. Lett.* **B356** (1995) 398;
S. Eidelman and F. Jegerlehner, *Z. Phys.* **C67** (1995) 585.

[9] S. Dittmaier, K. Kolodziej, M. Kuroda, and D. Schildknecht, *Nucl. Phys.* **B426** (1994) 249, E: **B446** (1995) 334.

[10] S. Dittmaier, M. Kuroda, and D. Schildknecht, *Nucl. Phys.* **B448** (1995) 3.

[11] L. Avdeev, J. Fleischer, S. Mikhailov and O. Tarasov, *Phys. Lett.* **B336** (1994) 560, E: **B349** (1995) 597;
K.G. Chetyrkin, J.H. Kühn and M. Steinhauser, *Phys. Lett.* **B351** (1995) 331.

[12] J.F. Grivaz, LAL-95-83, Proc. International EPS Conference on High-Energy Physics, Brussels, July 1995, eds. J. Lemonne, C. Vander Velde and F. Verbeure.

[13] G. Altarelli, R. Barbieri, and F. Caravaglios, *Phys. Lett.* **B349** (1995) 145.

[14] G. Altarelli, R. Barbieri and F. Caravaglios, CERN-TH-6859-93;
M. Shifman, *Mod. Phys. Lett.* **A10** (1995) 605.

[15] Particle Data Group, L. Montanet et al., *Phys. Rev.* **D50** (1994) 1173 and 1995 off-year partial update for the 1996 edition available on the PDG WWW pages (URL: http://pdg.lbl.gov/).

[16] S. Dittmaier, D. Schildknecht, and G. Weiglein, *Nucl. Phys.* **B465** (1996) 3; BI-TP 95/34, hep-ph/9511281.

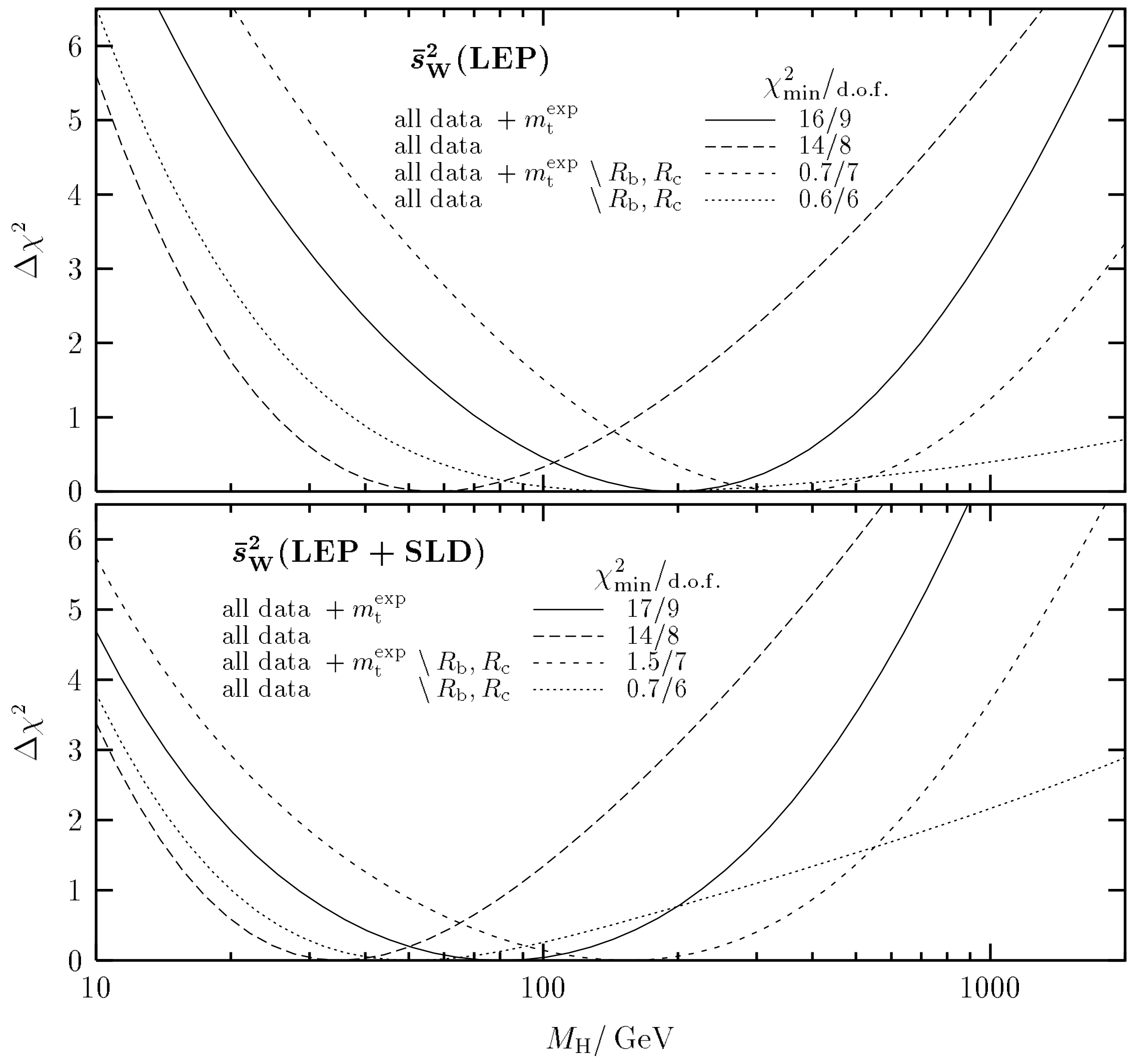

Figure 1: $\Delta\chi^2 = \chi^2 - \chi^2_{\rm min}$ is plotted against $M_{\rm H}$ for the $(m_{\rm t}, M_{\rm H}, \alpha(M_{\rm Z}^2), \alpha_{\rm s}(M_{\rm Z}^2))$ fit to various sets of physical observables, as specified in Tab. 2.

Figure 2: The results of the two-parameter $(m_{\rm t}, M_{\rm H})$ fits within the SM are displayed in the $(m_{\rm t}, M_{\rm H})$ plane. The three different columns refer to the three different sets of experimental data used in the corresponding fits,
(i) "leptonic sector": $\Gamma_{\rm l}, \bar{s}^2_{\rm W}({\rm LEP}), M_{\rm W}$,
(ii) "all data $\backslash R_{\rm c}, R_{\rm b}$": $\Gamma_{\rm T}, \Gamma_{\rm h}$ are added to set (i),
(iii) "all data $\backslash R_{\rm c}$": $\Gamma_{\rm T}, \Gamma_{\rm h}, \Gamma_{\rm b}$ are added to the set (i).
The second and the third rows show the shift resulting from changing $\alpha(M^2_{\rm Z})^{-1}$ and $\alpha_{\rm s}(M^2_{\rm Z})$, respectively, by one standard deviation in the SM prediction. The fourth row shows the effect of replacing $\bar{s}^2_{\rm W}({\rm LEP})$ by $\bar{s}^2_{\rm W}({\rm SLD})$ and $\bar{s}^2_{\rm W}({\rm LEP+SLD})$ in the fits. Note that the 1σ boundaries given in the first row are repeated identically in each row, in order to facilitate comparison with other boundaries. The value of $\chi^2_{\rm min}/_{\rm d.o.f.}$ indicated in the plots refers to the central values of $\alpha(M^2_{\rm Z})^{-1}$ and $\alpha_{\rm s}(M^2_{\rm Z})$. In all plots the empirical value of the top-quark mass (not included as input of the fits) of $m_{\rm t}^{\rm exp} = 180 \pm 12\,{\rm GeV}$ is also indicated.

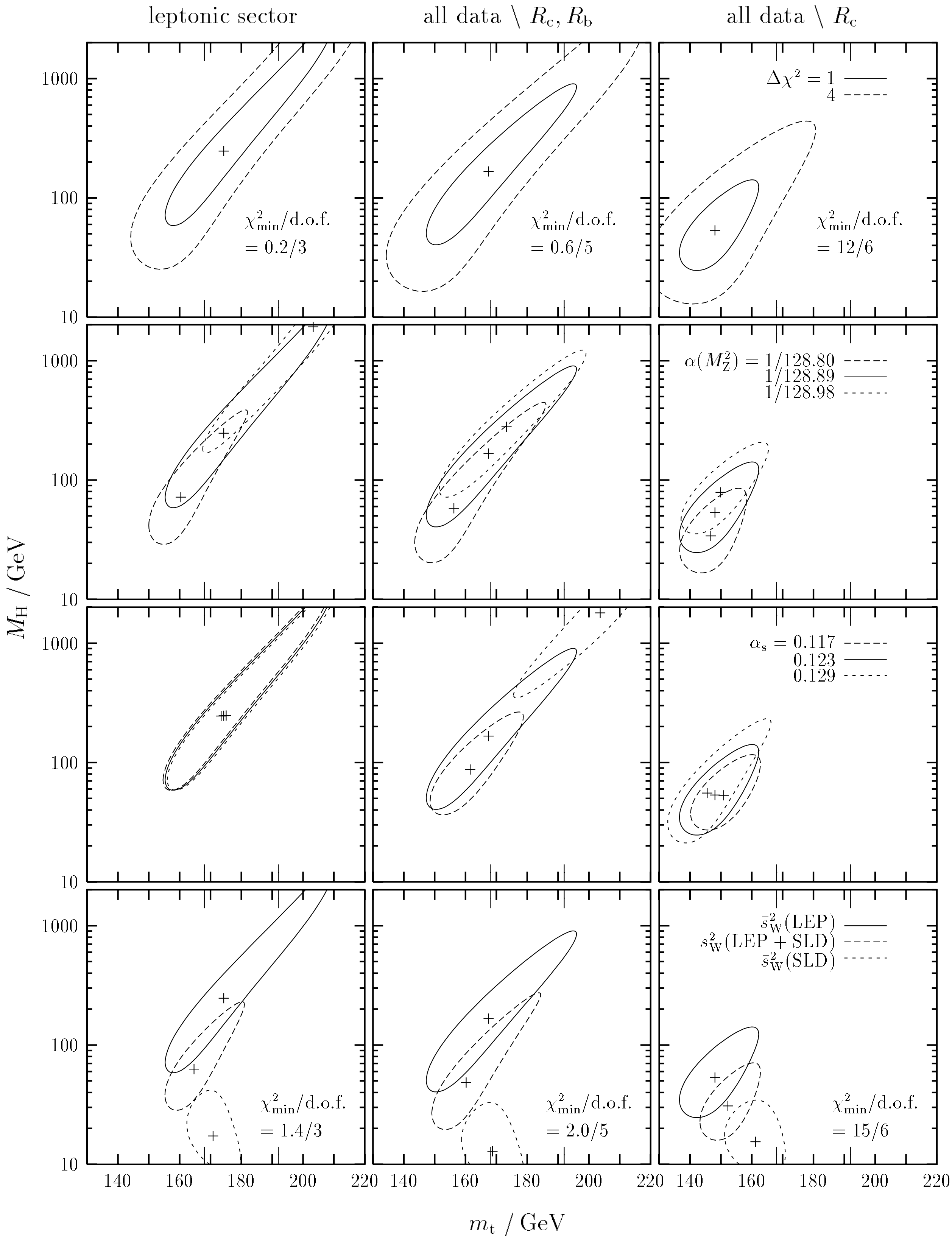
leptonic sector
all data \ R_c, R_b
all data \ R_c
$\Delta\chi^2 = 1$
4
χ^2_{min}/d.o.f. = 0.2/3
χ^2_{min}/d.o.f. = 0.6/5
χ^2_{min}/d.o.f. = 12/6
$\alpha(M_Z^2) = 1/128.80$
1/128.89
1/128.98
$\alpha_s = 0.117$
0.123
0.129
$\bar{s}^2_W$(LEP)
$\bar{s}^2_W$(LEP + SLD)
$\bar{s}^2_W$(SLD)
χ^2_{min}/d.o.f. = 1.4/3
χ^2_{min}/d.o.f. = 2.0/5
χ^2_{min}/d.o.f. = 15/6
M_H / GeV
m_t / GeV

Figure 2: